Shallow Water Propagation

William L. Siegmann
Rensselaer Polytechnic Institute
110 Eighth Street
Jonsson-Rowland Science Center 1C08
Troy, New York 12180-3590
phone: (518) 276-6905 fax: (518) 276-2825 email: siegmw@rpi.edu

Kara G. McMahon
Rensselaer doctoral student

Award Numbers: N000140410016
N000140910638 (Ocean Acoustics Graduate Traineeship)
http://www.math.rpi.edu/www/ocean_acoustics

LONG-TERM GOALS

Develop methods for deterministic and stochastic acoustic calculations in complex shallow water environments, specify their capabilities and accuracy, and apply them to explain experimental data and understand physical mechanisms of propagation.

OBJECTIVES

(A) Treat propagation from narrowband and broadband sources over elastic and poro-elastic sediments, and incorporate realistic bathymetric, topographic, and geoacoustic variations.

(B) Quantify acoustic interactions with physical features in the ocean volume and with geoacoustic features of the ocean sediment, and analyze and interpret experimental data.

APPROACH

(A) Develop efficient and accurate parabolic equation (PE) techniques for propagation through heterogeneous sediments. Treat range dependence and sediment layering by single scattering and energy conservation methods. Benchmark results using data and special high-accuracy solutions.

(B) Construct representations for ocean environmental and geoacoustic variability using data and parametric models. Determine acoustic fields with PE, normal mode, and other approximation methods. Use experimental data and computational results to assess propagation mechanisms.

- Principal collaborators are: Rensselaer PhD students, Dr. Michael Collins (NRL), Drs. James Lynch, Timothy Duda, and Ying-Tsong Lin (WHOI), Dr. Allan Pierce (BU, retired), and recent Rensselaer PhD graduates. Dr. William Carey (deceased) was an active collaborator.

Report Documentation Page

Form Approved
OMB No. 0704-0188

1. REPORT DATE	2. REPORT TYPE	3. DATES COVERED
2012	**N/A**	**-**

4. TITLE AND SUBTITLE	5a. CONTRACT NUMBER
Shallow Water Propagation	5b. GRANT NUMBER
	5c. PROGRAM ELEMENT NUMBER
6. AUTHOR(S)	5d. PROJECT NUMBER
	5e. TASK NUMBER
	5f. WORK UNIT NUMBER
7. PERFORMING ORGANIZATION NAME(S) AND ADDRESS(ES) **Rensselaer Polytechnic Institute 110 Eighth Street Jonsson-Rowland Science Center 1C08 Troy, New York 12180-3590**	8. PERFORMING ORGANIZATION REPORT NUMBER
9. SPONSORING/MONITORING AGENCY NAME(S) AND ADDRESS(ES)	10. SPONSOR/MONITOR'S ACRONYM(S)
	11. SPONSOR/MONITOR'S REPORT NUMBER(S)

12. DISTRIBUTION/AVAILABILITY STATEMENT
Approved for public release, distribution unlimited

13. SUPPLEMENTARY NOTES
The original document contains color images.

14. ABSTRACT

15. SUBJECT TERMS

16. SECURITY CLASSIFICATION OF:			17. LIMITATION OF ABSTRACT	18. NUMBER OF PAGES	19a. NAME OF RESPONSIBLE PERSON
a. REPORT	b. ABSTRACT	c. THIS PAGE			
unclassified	**unclassified**	**unclassified**	**SAR**	**12**	

WORK COMPLETED

(A) Propagation model development

(1) ***Accurate calculations range-dependent sediments and applications***

- High fidelity data from propagation over an elastic slab with variable bottom slopes in a NRL tank experiment validates accuracy [1] of a new PE method designed for problems with range-dependent bathymetry, variable thickness sediment layers, and topographic variations for applications to beach, island, and coastal problems.
- Additional verification of the method is obtained by comparing results [2] between accuracy benchmarks and computations for environments with large sound speeds changes and with waves on range-dependent elastic interfaces, and guidelines for choosing computational parameters are provided.
- An application of the new PE method is made to variable ice cover in polar regions [3], where particularly strong effects on transmission loss occur when the surface ice terminates and/or regenerates along the propagation direction.
- Another application is to shallow regions with partially consolidated sediment layers that are thin and have low shear speeds [4], which can treated by modeling the layers as transitional interfaces and enforcing suitable conditions.

(2) ***New calculations for elastic and poro-elastic sediments***

- Range-dependent transversely isotropic elastic sediments, which are a feature of many coastal regions, are treated by a PE new formulation [5] that enables evaluation of the relative significance of anisotropic effects on propagation.
- An initial propagation model that can treat weak range dependence in transversely isotropic poro-elastic sediments demonstrates that PE methods are feasible for these environments [6], and also indicates the influence of anisotropy.
- Propagation variables and computational techniques, developed for elastic sediments and designed for range-dependent layered environments, are generalized to multi-layered poro-elastic sediments [7], for which computational results agree with benchmarks for range-independent cases.

(B) Propagation mechanism assessment

(1) ***Nonlinear internal wave effects***

- If an acoustic mode propagates adiabatically across a nonlinear internal wave (NIW) at small incident angles with the wave front, the interaction may produce horizontal Lloyd mirror interference patterns [8], as predicted by other researchers and observed recently, and the patterns have especially interesting features when the NIW front has curvature.
- Parameters that characterize NIWs are estimated from satellite SAR images using edge identification and related techniques [9] in order to develop improved predictions of their acoustic effects, and parameter estimates are validated by comparisons with mooring and other available data.
- An adiabatic-mode transport theory is used to develop a scattering model for acoustic energy inside a NIW duct [10] in which wave front segments are treated as scattering elements, and a modified diffusion equation describes how averaged intensity evolves in the duct and depends on environmental and acoustic parameters.

- Calculations from the modal transport theory are used to determine how intersecting NIW fronts influence average intensity [11], depending on the orientations of the fronts and on the asymmetry of individual scattering elements.

(2) ***Propagation dependence on intrinsic sediment attenuation for sandy-silt sediments***

- A parametric description of simple shallow-ocean waveguides permits development of new approximations for modal attenuation coefficients [12], and their frequency behavior corresponds to that calculated for more complex waveguides.
- Comparisons between modal attenuation coefficients, obtained from Gulf of Mexico data and from new approximations [13], were performed after identifying a relevant subset of measured sound speed profiles, and the physical mechanism for the coefficient variations is explained.
- Modal attenuation coefficients and the overall attenuation of reduced transmission loss are examined [14] to reveal the influence of sound speed gradients at different locations in the water column and of sound speed profiles in the sediment.
- Relatively compact formulas for averaged transmission loss in range-independent waveguides are derived from mode theory [15], and they reduce to well-known results of Rogers and others for high frequencies and either isospeed or constant-gradient water sound speed profiles.

(3) ***Card-house structure theory for muddy sediments***

- One feature of this model is the presence of electric charges on bubbles, and under uniform conditions it is found that charged bubbles are required to be non-spherical [16], which has been observed in laboratory experiments and is anticipated for mud in situ.
- Another key model component is that based on their chemical, electrical, and material structure, mud platelets are hypothesized to behave like electric quadrupoles, so that estimates for shear wave speed are obtained [17] by computing the oscillation frequency of a hinged joint formed by two platelets which interact end to side.
- The shear speed calculation is extended to account for platelets for which the interaction is modeled as a cantilevered beam rather than a hinged joint [18], and estimates are consistent with low shear speed values found in high-porosity mud sediments.
- Estimates of another important mud parameter, porosity, are found by hypothesizing that mud platelets aggregate by an idealized process of fractal type [19], which is validated by finding a fractal dimension for the process and comparing with a result determined by an independent computation.

RESULTS (from two selected investigations)

(A) A critical capability for ocean acoustic data analysis and other applications is efficient and accurate propagation calculations in shallow water waveguides with range-dependent poro-elastic sediment layers. Porosity and elasticity are important physical mechanisms, because energy transfers between compressional and shear modes produce significant acoustic intensity and phase changes, and because attenuation may also increase substantially. A major computational challenge arises because wave number-energy spectra are much broader for poro-elastic sediments than for fluids. Our approach is based on the Biot poro-elastic theory, which is the most common model for ocean sediments. The only published poro-elastic PE appeared over a decade and a half ago, and even with an extension for sediment anisotropy [5], its computational capabilities are too limited for applications. It is essential that recent progress for elastic sediments be generalized to layered poro-elastic media. For example, one of the new methods has been validated with high quality data

from an NRL experimental series using elastic slabs [1] and with accurate computations for environments with range dependent interface waves [2]. These methods were developed from advances including formulations with different dependent variables, rotations of coordinates at range locations of bathymetry slope changes, and improved range-dependent corrections at stair-step approximations for ocean and sediment parameters. Last year we reported progress for the poro-elastic PE by generalizing its original variables to another set (denoted by $\hat{q}$), two of which appear in new elastic results. The top left panel in ***Figure 1*** illustrates that loss calculations for poro-elastic sediments with one or two layers can be drastically different. We found that the method is accurate for one-layer sediments; results are not displayed here. However, it is possible for accuracy to deteriorate unacceptably for two-layer sediments, as shown in the top right panel. This dilemma prompted a full reexamination of formulations for poro-elastic media, with the result that a new set of variables was devised for layered and range-dependent environments [7]. The middle panel shows calculations for a range-independent environment with the revised formulation (denoted by $\bar{q}$), along with a benchmark solution from the wavenumber integration code OASIS. The two curves are in excellent agreement. This example and others demonstrate that the $\bar{q}$ formulation produces accurate TL results for multi-layered poro-elastic media. Moreover, the formulation has capabilities which are needed for applications. The bottom left panel shows loss color contours for a source close to an interface between water and a poro-elastic sediment. A distinctive interference pattern produced by an interface wave and a water mode is apparent. The Scholte-like interface wave is directly analogous to the important Scholte wave at a water-elastic interface. This is shown by the bottom right panel, where a horizontal wave number spectrum indicates that the spectral position of the interface wave is near that of a true Scholte wave when the poro-elastic sediment becomes elastic. From these and other calculations, we conclude that the $\bar{q}$ PE solution has new capabilities for accurate propagation calculations in multi-layered poro-elastic environments. Future work includes improving capabilities, accuracy and efficiency for range-dependent problems, and additional benchmarking.

Figure 1 (next page). *Accurate calculation of propagation in layered poro-elastic sediments is obtained from an appropriate formulation of physical variables in the PE method. Two range-independent environments are described here, both having a 100 m isospeed ocean with c_w = 1500 m/s overlying a poro-elastic sediment. Environment A has a single deep layer with geoacoustic parameters: density solid ρ_s = 1.3 gm/cm^3, porosity α = 0.2, sound speeds c_{p1} = 1700 m/s, c_{p2} = 1250 m/s, and c_s = 800 m/s, and attenuations β_{p1} = 0.1 dB/λ , β_{p2} = 1 dB/λ , and β_s = 0.2 dB/λ . Environment B has a 20 m thick upper sediment layer that is the same as in Environment A and overlies a deep layer with geoacoustic paramters: ρ_s = 1.7 gm/cm^3, α = 0.2, c_{p1} = 2040 m/s, c_{p2} = 1250 m/s, c_s = 950 m/s, β_{p1} = 0.3 dB/λ , β_{p2} = 5 dB/λ , and β_s = 0.5 dB/λ . Higher values of β_{p2} reflect higher attenuations for the Biot slow compressional wave. In Figs. 1(a)-(c), transmission loss (TL) curves (dB re: 1 m) are shown between 30 and 90 dB along a 2 km track which is 75 m below the upper surface, for a 50 Hz source at 75 m depth.*

Fig. 1(a) *shows curves calculated by an earlier PE formulation with variables $\hat{q} = (u_x, w, \zeta)$, which generalize a successful elastic-media method. The dashed TL curve for Environment A shows a two-mode pattern, while the solid curve for Environment B shows one or more additional modes that produce a shorter pattern wavelength of about 300 m. The dissimilar TL curves mean that a single poro-elastic layer does not accurately represent an environment with two or more layers, when the upper layer is one wavelength thick. In* ***Fig. 1(b)*** *the solid TL curve is the same as in Fig. 1(a). The dashed curve also uses Environment B and is calculated from the wave number integration implementation OASIS. The curves have similar shapes but differ in amplitude and pattern phase.*

Fig. 1(c) *curves use the two-layer Environment B. They are plotted over a 5 km track and evolve to a three-mode pattern. The solid curve is calculated by a formulation with a new set of dependent variables $\bar{q} = (\Gamma, w, \Lambda)$, and the dashed curve is the solution from OASIS. The two curves are in excellent agreement and demonstrate that the new formulation produces accurate TL results for multi-layered poro-elastic media.*

Fig. 1(d) *illustrates that the new formulation has useful capabilities, such as calculating the influence of interface waves on TL. The same two-layer sediment Environment B is used with a 25 Hz source at 98 m, just above the interface. Color TL contours over 2 km in range and between 70 and 150 m depth are shown with a dynamic range of 40 dB. In addition to the mainly three-mode pattern, the contours show a rapid oscillation above and below 100 m from an interface wave.*

Fig. 1(e) *provides the horizontal wave number spectrum between 0.05 and 0.25 /m, normalized with maximum-peak amplitude one, for the calculation in Fig. 1(d) at a receiver depth 98 m. One large and two smaller peaks between 0.07 and 0.11 /m correspond to the three water modes, and another peak (with half the maximum amplitude) near 0.23 /m corresponds to the poro-elastic analog of a Scholte interface wave. This Scholte-like wave has a speed near 695 m/s, which is about 5% larger than the Scholte wave speed if the sediment is treated as elastic. From these and other calculations, we conclude that the $\bar{q}$ solution has the capability for accurate propagation calculations in multi-layered poro-elastic environments.*

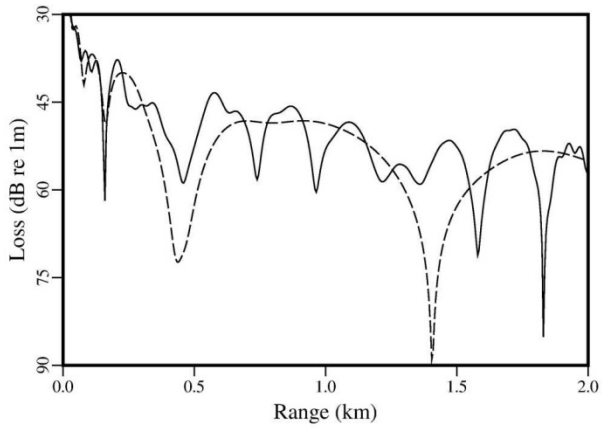
Loss (dB re 1m)
30
45
60
75
90
0.0
0.5
1.0
1.5
2.0
Range (km)

(a)

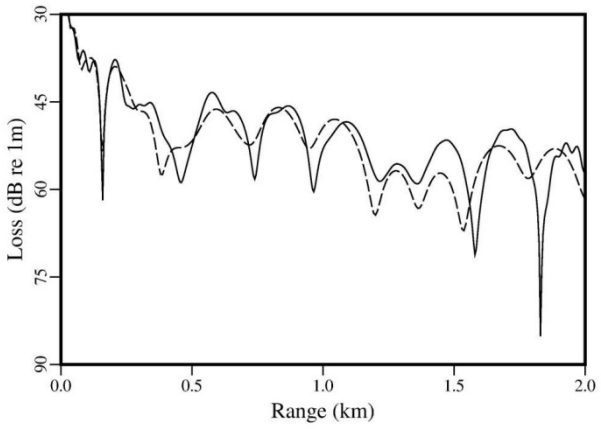
Loss (dB re 1m)
30
45
60
75
90
0.0
0.5
1.0
1.5
2.0
Range (km)

(b)

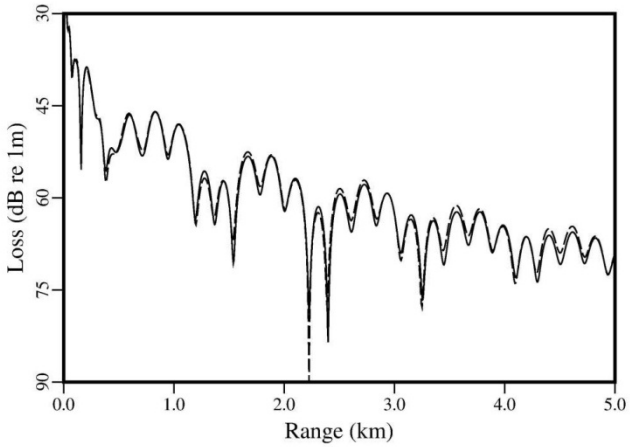
Loss (dB re 1m)
30
45
60
75
90
0.0
1.0
2.0
3.0
4.0
5.0
Range (km)

(c)

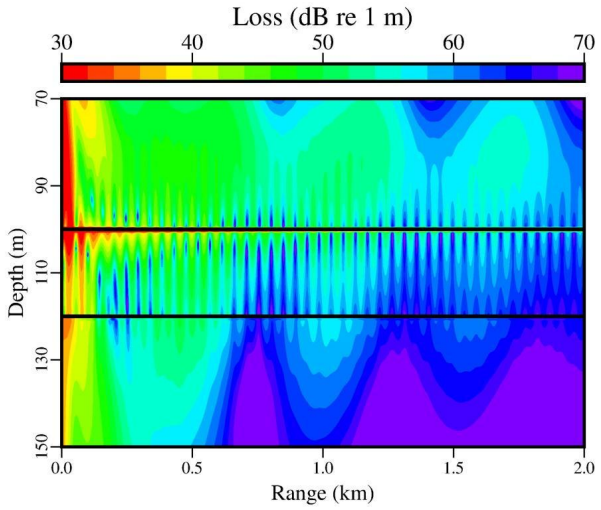
Loss (dB re 1 m)
30
40
50
60
70
Depth (m)
70
90
110
130
150
0.0
0.5
1.0
1.5
2.0
Range (km)

(d)

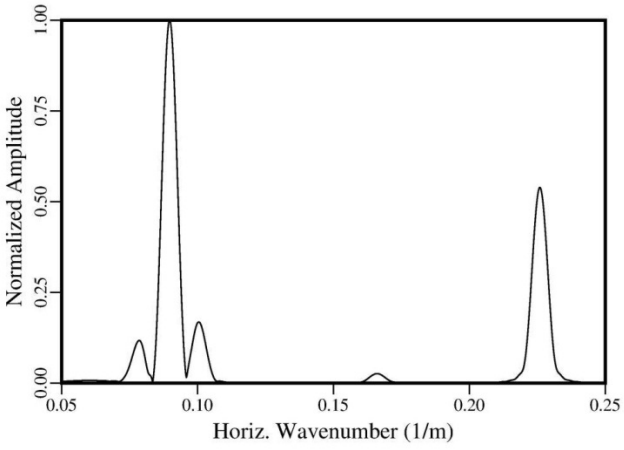
Normalized Amplitude
0.00
0.25
0.50
0.75
1.00
0.05
0.10
0.15
0.20
0.25
Horiz. Wavenumber (1/m)

(e)

(B) Both scientific understanding and specific knowledge of acoustic properties of shallow water bottoms are fundamental for many applications of interest. The widespread sandy-silt bottoms have received most attention and are handled effectively by elastic or Biot poro-elastic models. However, high-porosity seabed mud is different, because neither of these models correctly predicts or explains key geoacoustic properties of porosity, shear and compressional sound speeds, and attenuations. A card-house structure, recently proposed by Allan Pierce and William Carey, can potentially revolutionize approaches for treating mud bottoms. The structure relies on the fact that mineral components, which are in the form of thin platelets, have a particular distribution of electric charges that causes them to resemble small quadrupole sheets. This leads to repulsion for end-to-end or face-to-face contact and attraction between ends and faces, which in turn causes platelets to aggregate into structures of card-house form. The aggregates may have pores where bubbles of non-spherical shape can occur, and an initial explanation for such bubble shapes has been proposed [16]. In addition, different models for the electrical and mechanical interactions of platelets provide mechanisms for estimating shear speeds, depending on whether the platelets are predominantly rigid [17] or elastic [18]. Developments along these lines are critical to demonstrate the effectiveness of the card-house model for applications. In addition, the evolution and geometric properties of structures, and estimation of volume fractions of platelets and pores (porosity β), are themselves important to resolve. We considered known aggregation processes and concluded that for mud, the most likely is cluster-cluster aggregation constrained mainly by platelet diffusion. A collection of physically-based rules are hypothesized for such a process, along with several computational simplifications such as two-dimensional platelet interactions and horizontal or vertical platelet orientations. The top left panel of ***Figure 2*** illustrates a random initial distribution of platelets on a uniform rectangular grid with point spacing so that a platelet fits on three points. Computational iterations are performed that allow randomly selected platelets to translate or rotate. The top right panel, after 1000 iterations, shows clusters that have formed and suggests their increasing complexity as they interact. The lower left panel validates that the aggregation process has a fractal nature. The fractal dimension D should be the slope in a log-log plot of the number of platelets in a cluster versus an effective (dimensionless) cluster size, calculated from a radius of gyration. The slope $D = 1.60$ is significantly less than two which is the value for non-fractal behavior. The lower right panel involves the fractional solid content $1 - \beta$ of a cluster, calculated from a ratio of estimated solid and total areas. This log-log plot uses a specific combination as ordinate and the radius as abscissa in order that its slope is another estimate for $D = 1.56$. The closeness of the two D values is additional validation that the aggregation process is fractal. Moreover, if a selection is made for platelet aspect ratio, such as 0.05 for the mineral kaolinite, an estimate for porosity β is in the range $0.89 - 0.94$. This is consistent with accepted values near 0.90 for mud for which the card-house theory should apply. We conclude from these and other computations with the preliminary model that a fractal hypothesis for card-house aggregation is reasonable, and that estimates for fractal dimension are consistent with experimental observations. More importantly for geoacoustics, porosity estimates obtained from the computations are consistent with experimental observations. Future work includes relaxing constraints in the computational model, continuing the determination of porosity and sound speed, and specifying sensitivities of parameter estimates.

Figure 2 (next page). *The card-house theory for mud structure should permit estimates for key geoacoustic parameters such as porosity and shear sound speed. A computational approach based on modeling aggregation of platelets provides preliminary estimates of porosity. The mineral constituents of mud are modeled as thin platelets with length L, thickness h, and small aspect ratio $\delta = h/L$. Electrically they resemble quadrupoles that repel face-to-face and end-to-end but attract face-to-end. Aggregation is treated as a diffusion-limited cluster-cluster process that follows certain modeling rules, principally (1) interactions are two-dimensional, (2) platelets always lie horizontally or vertically on a uniform grid of points with spacing equal to L/2, (3) platelets move horizontally, vertically, or by rotating about their centers, (4) end-to-end and face-to-face platelet contact and overlapping platelets are forbidden, and (5) platelets undergoing center-to-end contact remain attached permanently.*

Fig. 2(a) *is an example of a random initial placement of nearly 1500 platelets, shown on a 40 by 40 grid with spacing 0.5 (all lengths in units of L). At this stage very few platelets have clustered. A series of iterations are performed, allowing randomly selected platelets to move up or down, or left or right, one grid spacing if feasible. Other randomly selected platelets perform a rotation of 90 degrees if feasible.* ***Fig. 2(b)*** *shows the result after 1000 iterations. A total of 17 clusters formed with a variety of sizes, several of which escaped the area shown. In the current version of the process, the clusters typically have pores that are accessible to the grid.*

Fig. 2(c) *is a demonstration of the fractal nature of the hypothesized aggregation process. A number of experimental investigations concluded that mud aggregates possess fractal geometry, with Minkowski-Bouligand (box counting) dimension of 1.5 or somewhat higher. A reasonable expectation is that a two-dimensional non-fractal cluster has dimensionless mass M satisfying $M \propto {R_g}^2$ where R_g is a calculated radius of gyration divided by L. Because the number N of platelets in a cluster is proportional to the dimensionless mass, $N \propto {R_g}^2$. These relations generalize to $M \propto {R_g}^D$ and $N \propto {R_g}^D$ for a fractal cluster, where D is the fractal dimension. The figure shows a plot of log N (from about 2.19 to 3.05) vs. log R_g (from about 0.69 to 1.20) for approximately three dozen aggregates, all of which were obtained from model computations and contain at least 150 platelets. The best fit line (solid red) has slope 1.60, which is an estimate for D that is consistent with previous work. A comparison line for non-fractal behavior (dashed blue) has slope 2.*

Fig. 2(d) *provides results for aggregate porosity β. The fractional solid content of a cluster, taken as proportional to its (dimensionless) density, is expected to satisfy the relation $1 - \beta \propto {R_g}^{D-2}$. The left side can be calculated by estimating solid and total areas for a cluster using a box counting procedure. It is worth noting from this relation that δ appears only in the proportionality factor, and consequently the exponent D is independent of δ. The figure shows a plot of log $((1 - \beta){R_g}^2)$ (from about 0.37 to 1.22) vs. log R_g (from about 0.69 to 1.20), which has a slope D = 1.56. The closeness of the two estimates for fractal dimension is important for the validity of the original hypothesis. With D given, porosity may be obtained by selecting a value for δ. For kaolinite platelets a typical value is $\delta = 0.05$, producing porosity estimates in the range $\beta = 0.89 - 0.94$. These are consistent with accepted values near 0.90 in mud for which the card-house theory should apply. We conclude from computations with this initial model version that a fractal hypothesis for card-house aggregation is reasonable and that estimates for fractal dimension are consistent with experimental observations. More importantly for geoacoustics, porosity estimates obtained from the model are consistent with experimental observations.*

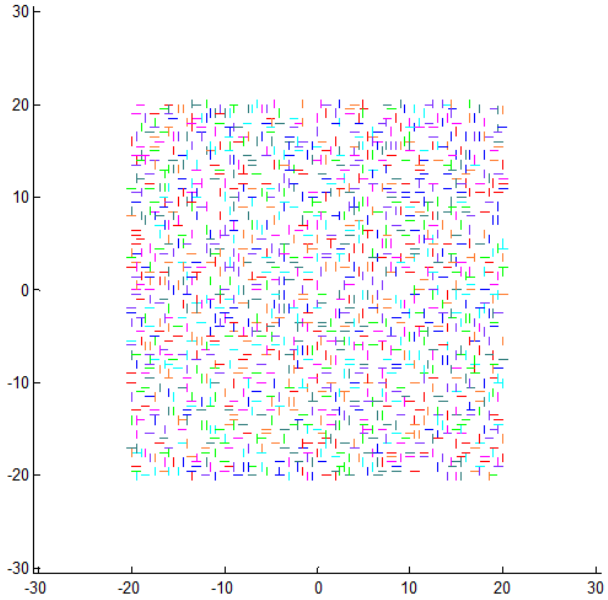
30
20
10
0
-10
-20
-30
-30
-20
-10
0
10
20
30

(a)

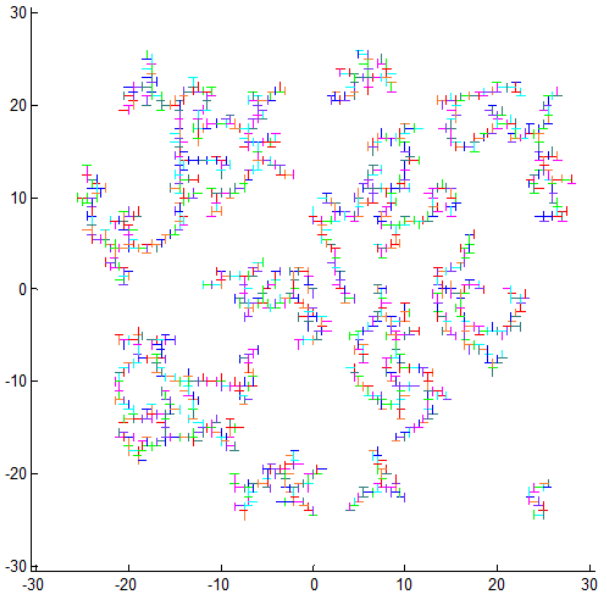
30
20
10
0
-10
-20
-30
-30
-20
-10
0
10
20
30

(b)

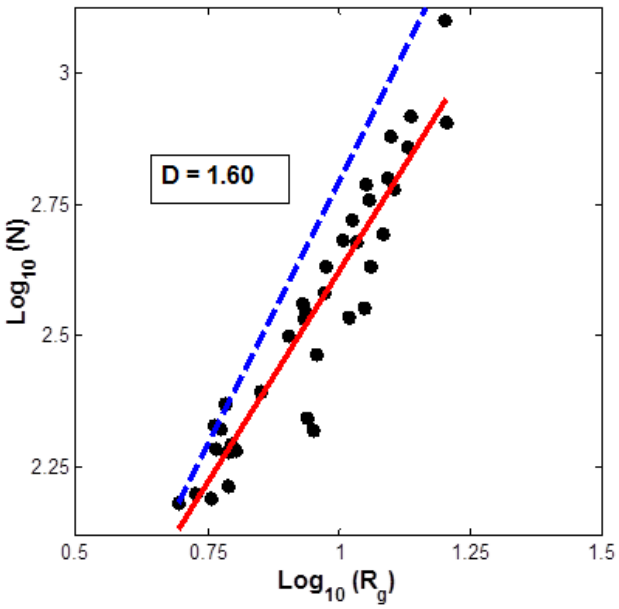
D = 1.60
Log10 (N)
Log10 (Rg)
3
2.75
2.5
2.25
0.5
0.75
1
1.25
1.5

(c)

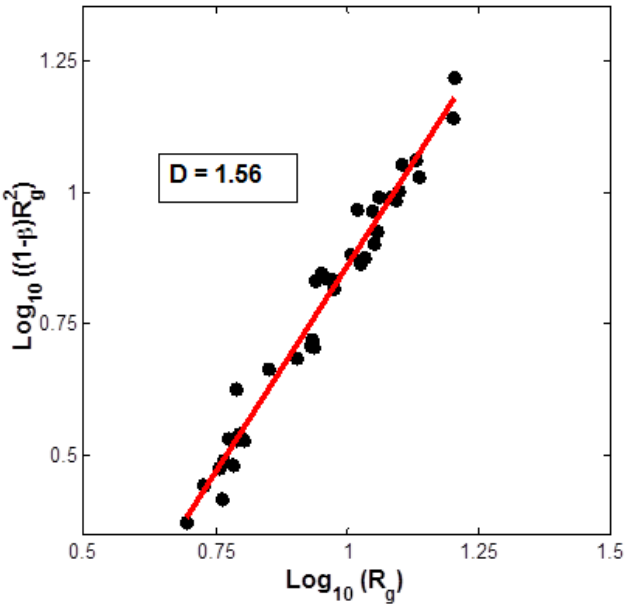
D = 1.56
Log10 ((1-μ)Rg2)
Log10 (Rg)
1.25
1
0.75
0.5
0.5
0.75
1
1.25
1.5

(d)

IMPACT/APPLICATIONS

New or enhanced capabilities are provided for propagation predictions that depend on physical properties of shallow water sediments, including layering, elasticity, porosity, and anisotropy. Range-dependent variability from bathymetry, topography, and sediment layer interfaces in propagation calculations can be treated. Intensity attenuation and coherence statistics that result from environmental fluctuations and other experimental variability can be found more efficiently. Data analyses and model comparisons allow specification for application purposes of the relative significance of key physical mechanisms: linear versus nonlinear frequency dependence of sediment attenuation, sediment heterogeneity versus homogeneity, water column versus bathymetric variability, water column scattering versus refraction, and vertical versus horizontal mode coupling due to nonlinear internal waves and bathymetry. Results from modeling and data analyses of experiments, particularly experiments off the New Jersey Shelf, are partly aimed toward improving shallow water sonar systems and predictions. Propagation model implementations, analysis tools, and data representation techniques are distributed to university, laboratory, and research/development groups.

RELATED PROJECTS

- Continuing projects with Dr. Michael Collins include [5] and a monograph on new parabolic wave equation models and applications [21], for which the principal research results are nearly complete and chapter drafts are prepared.

- In addition to investigations with Drs. James Lynch, Timothy Duda, and Y.-T. Lin and their colleagues [9]-[11] of propagation effects from waveguides of variable structure generated by nonlinear internal waves, a related project characterizes whispering gallery and other modes [20].

- Research with Dr. Allan Pierce [15]-[19] focuses on propagation variability from sediment geoacoustic structure and attenuation and on quantifying predictions from his card-house theory of mud structure and acoustics.

REFERENCES

[1] H. J. Simpson, J. M. Collis, R. J. Soukup, M. D. Collins, and W. L. Siegmann, "Experimental testing of the variable rotated elastic parabolic equation," *J. Acoust. Soc. Am.*, **130**, 2681-2686 (2011).

[2] A. M. Metzler, W. L. Siegmann, M. D. Collins, and J. M. Collis, "Single-scattering parabolic equation solutions for elastic media propagation, including Rayleigh waves," *J. Acoust. Soc. Am.,* **131**, 1131-1137 (2012).

[3] A. M. Metzler, J. M. Collis, and W. L. Siegmann, "Low-frequency seismo-acoustic propagation under variable ice over in the Arctic using a parabolic equation." See also (A) *J. Acoust. Soc. Am.,* **132**, 1974 (2012). In preparation for submission.

[4] J. M. Collis, A. M. Metzler, and W. L. Siegmann, "Seismo-acoustic propagation for thin and low shear speed ocean elastic sediments." See also (A) *J. Acoust. Soc. Am.,* **132**, 1973 (2012). In preparation for submission.

[5] A. M. Metzler, W. L. Siegmann, M. D. Collins, and J. M. Collis, "Parabolic equation solutions for anisotropic waves in heterogeneous media." See also (A) *J. Acoust. Soc. Am*. **125**, 2500 (2009). In preparation for submission.

[6] A. J. Fredricks, W. L. Siegmann, and M. D. Collins, "Parabolic equation models for anisotropic poro-elastic media." Submitted for refereed publication.

[7] A. M. Metzler, W. L. Siegmann, M. D. Collins, and J. M. Collis, "Improved parabolic equation solution for layered poro-elastic media." See also (A) *J. Acoust. Soc. Am*. **127**, 1962 (2010). Submitted for refereed publication.

[8] K. G. McMahon, L. K. Reilly-Raska, W. L. Siegmann, J. F. Lynch, and T. F. Duda, "Horizontal Lloyd Mirror patterns from straight and curved nonlinear internal waves," *J. Acoust. Soc. Am.*, **131**, 1689-1700 (2012). Supported by OA Graduate Traineeship Award 0638.

[9] C. C. Boughan Khan, T. F. Duda, J. F. Lynch, A. E. Newhall, and W. L. Siegmann, "Nonlinear internal wave parameter extraction from SAR images." In preparation for submission.

[10] K. G. McMahon, J. F. Lynch, Y.-T. Lin, W. L. Siegmann, and N. Xiang, "Energy transport in nonlinear internal wave ducts." See also (A) *J. Acoust. Soc. Am*. **128**, 2335 (2010). In preparation for submission. Supported by OA Graduate Traineeship Award 0638.

[11] K. G. McMahon, Y.-T. Lin, J. F. Lynch, and W. L. Siegmann, "Energy transport in intersecting nonlinear internal wave ducts." See also (A) *J. Acoust. Soc. Am*. **129**, 2458 (2011). In preparation for submission. Supported by OA Graduate Traineeship Award 0638.

[12] W. J. Saintval, A. D. Pierce, W. M. Carey, and W. L. Siegmann, "A modified Pekeris waveguide for examining sediment attenuation influence on modes." Submitted for refereed publication.

[13] W. J. Saintval, W. L. Siegmann, W. M. Carey, and A. D. Pierce, "Parameter sensitivities of modal attenuation coefficients for sandy sediments in the Gulf of Mexico." Submitted for refereed publication.

[14] W. J. Saintval, S. V. Kaczkowski, W. L. Siegmann, W. M. Carey, A. D. Pierce, and J. F. Lynch, "Parameter variability of modal attenuation coefficients and averaged transmission loss attenuation obtained from modal approximations." In preparation for submission.

[15] S. V. Kaczkowski, A. D. Pierce, W. M. Carey, and W. L. Siegmann, "Averaged transmission loss expressions in shallow water waveguides with sandy-silty sediments." See also (A) *J. Acoust. Soc. Am*. **128**, 2480 (2010). In preparation for submission.

[16] J. O. Fayton, A. D. Pierce, W. M. Carey, and W. L. Siegmann, "The card-house structure of mud: Influence of particle interaction energy on bubble formation and growth." See also (A) *J. Acoust. Soc. Am*. **127**, 1938 (2010). In preparation for submission.

[17] J. O. Fayton, A. D. Pierce, W. M. Carey, and W. L. Siegmann, "The card-house structure of mud: Determination of shear wave speed." See also (A) *J. Acoust. Soc. Am*. **128**, 2357 (2010). In preparation for submission.

[18] J. O. Fayton, A. D. Pierce, W. M. Carey, and W. L. Siegmann, "The card-house structure of mud: Estimation of shear wave speed in mud with elastic platelets." See also (A) *J. Acoust. Soc. Am*. **129**, 2389 (2011). In preparation for submission.

[19] J. O. Fayton, W. M. Carey, A. D. Pierce, and W. L. Siegmann, "The card-house structure of mud: Estimation of porosity from computational fractal modeling." In preparation for submission.

[20] Y.-T. Lin, K. G. McMahon, W. L. Siegmann, and J. F. Lynch, "Horizontal ducting of sound by curved nonlinear internal gravity waves in the continental shelf areas." Submitted for refereed publication. Supported by OA Graduate Traineeship Award 0638.

[21] M. D. Collins and W. L. Siegmann, *Parabolic Wave Equations with Applications*. In preparation for Springer-Verlag publishers.

PUBLICATIONS

- Published [refereed]: [1], [2], [8]
- Submitted [refereed]: [6], [7], [12], [13], [20]